A. N. Norris

D. A. Rebinsky

Department of Mechanical and Aerospace Engineering, Rutgers University, Piscataway, NJ 08855-0909

Membrane and Flexural Waves on Thin Shells

Membrane and flexural waves are limiting short wavelength solutions of the equations of motion for arbitrarily curved, smooth shells. Each distinct wave type is found using a geometrical or ray method based upon asymptotics in the small parameters h/R, where h is thickness and R a minimum radius of curvature. Useful, asymptotic formulae are found for the normal displacement associated with membrane waves, group velocities, and other physically significant quantities. Ray paths on a conical shell are illustrated for each wave type, and it is found that flexural rays form a caustic near the vertex.

1 Introduction

Normal mode descriptions of shell dynamics become very cumbersome at high frequencies, where it is more profitable to consider local wave effects on the structure. From this viewpoint the motion of the shell is the superposition of distinct wave types, just as the motion of an isotropic elastic solid can be locally decomposed into compressional and shear waves. The decomposition is rigorous in the latter case, but is necessarily approximate for thin shells with non-zero Gaussian curvature. However, the idea of waves traveling along rays on the shell is conceptually appealing and simplifies our physical understanding of the mechanisms for energy transport. For instance, recent experiments on the nearfield acoustics of submerged thin shells have been interpreted using similar ideas (Williams et al., 1990).

Several authors have employed the methods of geometrical acoustics to analyze shell dynamics, including Ross (1968) who considered axisymmetric motions, and Germogenova (1973) who focused on flexural wave solutions. Pierce (1989) and Pierce and Kil (1990) have shown that the Donnell equations for a cylindrical shell are similar to those describing structural wave disturbances in a two-dimensional unbounded homogeneous anisotropic medium. Therefore, one can apply results and concepts for waves in anisotropic media to shell dynamics. Recently, Pierce (1992a) has developed a fairly general theory for waves of short wavelength propagating over thin shells of arbitrary shape. The principal restriction is that the wavenumber must be large compared with the two principal curvatures. Pierce's theory predicts both dispersion and anisotropy, the latter dependent upon the orientation of the propagation direction with the local directions of principal curvature.

The focus of this paper is on developing the methods of geometrical acoustics for wave propagation over the surface of a shell of arbitrary shape. We use the formalism of ray theory and the eiconal equation as developed by Keller (1978) for general wave problems; however, our work is strongly influenced by recent work along these lines by Pierce (1992a).

Contributed by the Technical Committee on Vibration and Sound for publication in the JOURNAL OF VIBRATION AND ACOUSTICS. Manuscript received Nov. 1992; revised May 1993. Associate Technical Editor: S. C. Sinha.

Separate analyses are performed to extract the governing behavior of flexural and membrane waves. Our method of analysis emphasizes the fact that the separate wave types correspond to distinct asymptotic scalings. This leads to some simplification in the dispersion relations, and greatly simplifies the task of finding the polarization vectors and group velocities. In the following sections we assume a short wavelength asymptotic expansion using a general ansatz specifically tailored for flexural or membrane waves. These asymptotic approximations are applied to the general equations describing a shell of arbitrary shape under fluid loading, which are summarized in Section 2. The asymptotic scalings are discussed in Section 3, and applied to membrane and flexural waves in Sections 4 and 5, respectively. In each case we discuss the dispersion relation, the group velocities and the polarizations of the tangential and normal displacements. The general theory for an arbitrary shell is applied to conical shells in Section 6, where we also provide illustrations of flexural and membrane ray paths near the vertex of a cone.

2 Thin Shell Theory

The tensor form of the equations summarized here follows from the works of Green and Zerna (1968), Koiter (1960) and Pierce (1992a,b), and are consistent with the theories of each author. A good review of thin shell theories can be found in the monograph of Leissa (1973). The equations are for an arbitrarily curved, smooth shell and include both membrane and bending effects. It is assumed that the shell is thin, i.e., $h \ll R_{min}$, where h is the thickness and R_{min} the smallest principal radius of the undeformed middle surface, and that stress is approximately plane, i.e., the traction normal to the undeformed middle surface is small in comparison with the remaining in-plane components of stress. The asymptotics in Section 3 are premised upon the assumption that the wavelengths of interest are much shorter than R_{min} ; however, at the same time they must be much longer than h, i.e., thin shell theory requires that the frequency is restricted to $\Omega h \ll 1$, where Ω is defined in Eq. (8a). The curvilinear coordinates on the shell are θ^1 and θ^2 , with corresponding direction vectors \mathbf{a}_{∞}

 $= \mathbf{x}_{,\alpha}$, $\alpha = 1$, 2, and surface normal $\mathbf{a}_3 = \mathbf{a}_1 \wedge \mathbf{a}_2 / |\mathbf{a}_1 \wedge \mathbf{a}_2|$ directed out of the shell. In general, greek sub- or superscripts assume the values 1 or 2, and the suffix, α denotes differentiation with respect to θ^{α} . The surface metric tensor has components $a_{\alpha\beta} = \mathbf{a}_{\alpha} \cdot \mathbf{a}_{\beta}$, and the curvature tensor is $d_{\alpha\beta} = \mathbf{a}_{\alpha} \cdot \mathbf{a}_{\beta}$. Vectors are defined relative to these tangent vectors by their components, e.g., $\mathbf{k} = k^{\alpha}\mathbf{a}_{\alpha}$. Components are raised and lowered by the metric tensor; thus $v_a = a_{\alpha\beta}v^{\beta}$, and $a_{\alpha\gamma}a^{\gamma\beta} = \delta^{\alpha}_{\alpha}$. The squared magnitude of a vector is $k^2 = k^{\alpha}k_{\alpha} = k^{\alpha}k^{\beta}a_{\alpha\beta} = k_{\alpha}k_{\beta}a^{\alpha\beta}$. The covariant derivative of a scalar is $D_{\alpha}w = w_{,\alpha}$, and for vector components $D_{\beta}v^{\alpha} = v^{\alpha}_{,\beta} + \Gamma^{\alpha}_{\beta\gamma}v^{\gamma}$, or $D_{\beta}v_{\alpha} = v_{\alpha,\beta} - \Gamma^{\gamma}_{\alpha\beta}v_{\gamma}$, where the Christoffel symbols are defined as $\Gamma^{\alpha}_{\beta\gamma} = a^{\alpha\lambda} \mathbf{a}_{\lambda} \cdot \mathbf{a}_{\beta,\gamma}$.

The displacement vector of a point originally on the middle surface is decomposed into tangential and normal components as $\mathbf{u} = v^{\alpha} \mathbf{a}_{\alpha} + w \mathbf{a}_{3}$. The equilibrium equations for a thin shell subject to fluid loading are

$$\rho h \frac{\partial^2 v^{\alpha}}{\partial t^2} = D_{\beta} n^{\alpha \beta}, \quad \alpha = 1, 2, \tag{1a}$$

$$\rho h \frac{\partial^2 w}{\partial t^2} = D_{\alpha} q^{\alpha} - n^{\alpha \beta} d_{\alpha \beta} - p_{\text{dif}}, \tag{1b}$$

where $p_{\rm dif}=p_+-p_-$ is the difference between the acoustic pressures on the exterior and interior of the shell and ρ is the mass density per unit volume of the solid. Also, $n^{\alpha\beta}$ and $m^{\alpha\beta}$ are the in-plane stress resultants and the stress couples, respectively, and the shearing forces q^{α} are related to the couples by $q^{\alpha}=D_{\beta}m^{\alpha\beta}$. The constitutive relations for an elastic shell are

$$n^{\alpha\beta} = C H^{\alpha\beta\rho\lambda} e_{\rho\lambda}, \quad m^{\alpha\beta} = -B H^{\alpha\beta\rho\lambda} D_{\rho} D_{\lambda} w$$
 (2)

where the in-surface strains are $e_{\alpha\beta} = (a_{\beta\gamma}D_{\alpha}v^{\gamma} + a_{\alpha\gamma}D_{\beta}v^{\gamma})/2 + d_{\alpha\beta}w$. The tensor **H** depends upon the symmetry of the material comprising the shell, and simplifies for isotropic materials of Poisson's ratio ν to

$$H^{\alpha\beta\rho\lambda} = \frac{1}{2}(1 - \nu)(a^{\alpha\lambda}a^{\beta\rho} + a^{\alpha\rho}a^{\beta\gamma}) + \nu \ a^{\alpha\beta}a^{\rho\lambda}. \tag{3}$$

The parameters $C = Eh/(1 - v^2)$ and $B = Eh^3/(1 - v^2)$ are the extensional and bending stiffness, respectively, where E is the Young's modulus. In summary, the equations of motion for an isotropic shell may be written,

$$\rho h \frac{\partial^2 v^{\alpha}}{\partial t^2} = D_{\beta} \{ C[(1-\nu)e^{\alpha\beta} + \nu e_{\gamma}^{\gamma} a^{\alpha\beta}] \}, \quad \alpha = 1, 2, \quad (4a)$$

$$\rho h \frac{\partial^2 w}{\partial t^2} = -D_{\alpha} D_{\beta} [B(1-\nu)D^{\alpha}D^{\beta}w] - D_{\alpha}D^{\alpha} [B\nu D_{\beta}D^{\beta}w] - C[(1-\nu)d^{\alpha}_{\beta}e^{\beta}_{\alpha} + \nu d^{\alpha}_{\alpha}e^{\beta}_{\beta}] - p_{\text{dif}}.$$
 (4b)

3 Short Wavelength Asymptotics

We consider solutions of the form

$$\mathbf{u}(\mathbf{x}, t) = \mathbf{u}^{(\epsilon)}(\mathbf{x}, t) \exp\{i\epsilon^{-\lambda}\phi(\mathbf{x}, \epsilon^{\mu}t)\}, \tag{5}$$

where $\phi(x, t)$ is the *phase function* and ϵ is a small parameter, $\epsilon << 1$. The choice of the parameters $\lambda \geq 0$ and $0 \leq \mu \leq \lambda$ determines the wave type, flexural or membrane. Define the frequency ω and surface wave number vector \mathbf{k} ,

$$\omega = -\phi_{,t}(\mathbf{x}, \, \epsilon^{\mu}t), \quad k_{\alpha} = D_{\alpha}\phi(\mathbf{x}, \, \epsilon^{\mu}t). \tag{6}$$

The actual surface wavenumber is not k but $e^{-\lambda}$ k, which depends upon the choice of λ . After performing the asymptotic scaling we will set $\lambda = 0$ and $\mu = 0$ (or equivalently set $\epsilon \to 1$) so that there is no distinction between the two. The same goes for the frequency ω . It is useful to consider the small parameter to be defined by

$$\epsilon = \sqrt{h/R} \tag{7}$$

where R is a fixed but arbitrary length, such as a typical radius of curvature. The arbitrary nature of R means that it may be identified with the radius of curvature for the purposes of scaling, but may be set equal to h after the scaling is performed, thus eliminating the explicit dependence upon ϵ .

We also define the following parameters,

$$\Omega = \omega/c_p, \tag{8a}$$

$$\Omega_{\rm ring}^2 = \frac{1}{R_I^2} + \frac{1}{R_{II}^2} + \frac{2\nu}{|R_I R_{II}|},\tag{8b}$$

where R_I and R_{II} are the principal radii of curvature, and c_p is the longitudinal plate wave speed, $c_p^2 = E/(1 - \nu^2)\rho$. We will also need the shear speed c_s , where $c_s^2 = E/2(1 + \nu)\rho$, and the tensors

$$F_{\beta}^{\alpha} = \frac{1}{2} (1 - \nu) k^2 a_{\beta}^{\alpha} + \frac{1}{2} (1 + \nu) k^{\alpha} k_{\beta}, \tag{9a}$$

$$G_{\beta}^{\alpha} = (1 - \nu)d_{\beta}^{\alpha} + \nu d_{\gamma}^{\gamma} a_{\beta}^{\alpha}. \tag{9b}$$

Define the perpendicular wavenumber vector as $\mathbf{k}^{\perp} = \mathbf{a}_3 \wedge \mathbf{k}$. Hence, if $\mathbf{k} = (k_I, k_{II})$ in principal curvature coordinates, then $\mathbf{k}^{\perp} = (-k_{II}, k_{I})$. Finally, define the unit vector in the direction of the wavenumber vector as $\mathbf{n} = \mathbf{k}/k$, also known as the wavenumal, and $\mathbf{n}^{\perp} = \mathbf{a}_3 \wedge \mathbf{n}$.

For fluid loading on the outside only we have $p_{-} = 0$, and we assume a local fluid loading impedance, Z_{rad} , such that

$$p_{+} = -i\omega Z_{rad}w. ag{10}$$

However, we do not assume any specific form for the radiation impedance in this paper, but refer to Junger and Feit (1986) and Pierce (1992a) for further details. It helps to define a nondimensional impedance,

$$\hat{Z}_{rad} = \frac{Z_{rad}}{-i\omega\rho h},\tag{11}$$

where the appearance of h in \hat{Z}_{rad} suggests that it should be scaled with ϵ . The appropriate scaling turns out to be

$$\hat{Z}_{rad} = \epsilon^{2(\mu - \lambda)} \hat{Z}_{rad}^{o}, \tag{12}$$

where \hat{Z}_{rad}^o is assumed to be a quantity of order unity. We will see in the next sections that this scaling is indeed the correct one which includes fluid loading effects in membrane and flexural waves.

3.1 Pierce's Dispersion Relation. Pierce (1992a) derived a general dispersion relation based upon an assumed form similar to Eq. (5), with $\epsilon=1$ and $\mathbf{u}^{(\epsilon)}=\hat{\mathbf{u}}$, where $\hat{\mathbf{u}}$ is constant. The main assumption was that the wavenumber vector \mathbf{k} is large in comparison with inverse lengths of the order 1/R, where R is a typical radius of curvature. No explicit assumption was made about the magnitude of the frequency ω , although there appears to be a slight inconsistency on this point, which we will discuss below. By substituting this ansatz into the equation of motion, Pierce obtained the 3×3 eigenvalue system

$$(F^{\alpha}_{\beta} - \Omega^{2} a^{\alpha}_{\beta}) \hat{v}^{\beta} - iG^{\alpha}_{\beta} k^{\beta} \hat{w} = 0, \qquad (13a)$$

$$-iG^{\alpha}_{\beta}k_{\alpha}\hat{v}^{\beta} + \left(\Omega^2 - \frac{1}{12}h^2k^4 - \Omega^2_{ring} - \Omega^2\hat{Z}_{rad}\right)\hat{w} = 0. \quad (13b)$$

The dispersion relation follows by setting the determinant of the 3×3 matrix to zero. The procedure for simplifying this is explained in detail by Pierce (1992a), with the final result given in Eq. (43) of his paper. We present here the same dispersion relation but in a slightly simpler form:

$$\left(\Omega^{2} - \frac{1 - \nu}{2} k^{2}\right) \left[(\Omega^{2} - k^{2}) \left(\Omega^{2} (1 + \hat{Z}_{rad}) - \frac{h^{2}}{12} k^{4}\right) - \Omega^{2} \Omega_{ring}^{2} \right]
= -(1 - \nu^{2}) \left[\Omega^{2} \left(\frac{k_{I}^{2}}{R_{II}^{2}} + \frac{k_{II}^{2}}{R_{I}^{2}}\right) - \frac{1 - \nu}{2} \left(\frac{k_{I}^{2}}{R_{II}} + \frac{k_{II}^{2}}{R_{I}}\right)^{2} \right].$$
(14)

Note that the left member is isotropic as it depends upon k only through its magnitude, but the right member is anisotropic.

The dispersion relations that we obtain in the next sections are approximations of this general relation under the scalings appropriate to the wave types. For membrane waves, longitudinal and shear, the frequency and wavenumber are of the same order and large, whereas for the flexural wave the wavenumber is large but the frequency may be of order unity. These distinctions arise from different choices of the numbers λ and μ in Eq. (5), and also require appropriate scaling of the displacement components in terms of ϵ , as discussed below. The eigenvalue problem, Eqs. (13), from which Eq. (14) is derived explicitly includes the frequency terms in the membrane equations, but ignores other terms of order k that appear in the exact equations. In effect, the resulting dispersion relation is only valid for frequencies Ω such that the wavenumber k is large, which turns out to be the case for membrane waves when the frequency is also large. For flexural waves it is possible to get large k for Ω of order unity. In both these cases, one can simplify the roots of the dispersion relation (14) by approximations.

4 Membrane Waves

4.1 The Dispersion Relation. Let $\mu=0$, $\lambda>0$ in Eq. (5), and assume the following ansatz for the displacement components,

$$v^{(\epsilon)\alpha}(\mathbf{x}, t) = V^{\alpha}(\mathbf{x}, t) + \epsilon^{\lambda} \hat{V}^{\alpha}(\mathbf{x}, t) + \dots, \qquad (15a)$$

$$w^{(\epsilon)}(\mathbf{x}, t) = \epsilon^{\lambda} W(\mathbf{x}, t) + \epsilon^{2\lambda} \hat{W}(\mathbf{x}, t) + \dots, \qquad (15b)$$

If these are substituted into the w equation, Eq. (4b), it is clear that the bending terms are of smaller order if $0 < \lambda < 2$. We therefore assume that $\lambda = 1$, in which case the w equation implies

$$W = \frac{i}{\Omega^2} (1 + \hat{Z}_{rad}^{\circ})^{-1} G_{\beta}^{\alpha} k_{\alpha} V^{\beta}.$$
 (16)

Next, substitute Eqs. (5) and (15a) into Eq. (4a) and keep only the leading order coefficients of V^{α} and W, yielding

$$\Omega^2 V^{\alpha} - F^{\alpha}_{\beta} V^{\beta} + i \epsilon^2 G^{\alpha}_{\beta} k^{\beta} W = 0.$$
 (17)

The appearance of ϵ^2 means that the curvature is asymptotically negligible for the leading order membrane waves. However, it is useful to maintain this term in the analysis of the dispersion relation to see what is the first, albeit small, influence of curvature.

Eliminating W from Eqs. (16) and (17) gives

$$\left\{ \Omega^2 \ a^{\alpha}_{\beta} - F^{\alpha}_{\beta} - \frac{\epsilon^2}{\Omega^2} \frac{G^{\alpha}_{\gamma} G^{\alpha}_{\beta} k^{\gamma} k_{\lambda}}{(1 + \hat{Z}^{o}_{rad})} \right\} \ V^{\beta} = 0.$$
 (18)

The dispersion relation follows from the condition that this system has nontrivial solution, implying that the determinant of the matrix must vanish. It is possible to expand the determinant by expressing the matrix elements in terms of the principal coordinates. After some algebra, similar to the algebra leading to Eq. (14), we find

$$(\Omega^{2} - k^{2}) \left(\Omega^{2} - \frac{1 - \nu}{2} k^{2}\right) - \frac{\epsilon^{2}}{\Omega^{2}(1 + \hat{Z}_{rad}^{o})} \left\{k^{2} \Omega_{ring}^{2} \left(\Omega^{2} - \frac{1 - \nu}{2} k^{2}\right)\right\}$$

$$-(1-\nu^2)\left[\Omega^2\left(\frac{k_I^2}{R_{II}^2} + \frac{k_{II}^2}{R_I^2}\right) - \frac{1-\nu}{2}\left(\frac{k_I^2}{R_{II}} + \frac{k_{II}^2}{R_I}\right)^2\right]\right\} = 0. \quad (19)$$

The leading order roots of this equation ($\epsilon=0$) give the nondispersive longitudinal and shear wave modes found in the theory of thin plates. The first curvature corrections follow by expanding the roots for $\epsilon<<1$, retaining the first additional terms, and finally set $\epsilon=1$ which is equivalent to unscaling, to get

$$k^{2} = \begin{cases} \Omega^{2} - \frac{1}{1 + \hat{Z}_{rad}} \left[\left(\frac{n_{I}^{2}}{R_{I}} + \frac{n_{II}^{2}}{R_{II}} \right) + \nu \left(\frac{n_{II}^{2}}{R_{I}} + \frac{n_{I}^{2}}{R_{II}} \right) \right]^{2} + O\left(\frac{1}{\Omega^{2}} \right), \\ &: \text{longitudinal,} \\ \frac{2}{(1 - \nu)} \Omega^{2} - \frac{(2n_{I}n_{II})^{2}}{1 + \hat{Z}_{rad}} \left(\frac{1}{R_{I}} - \frac{1}{R_{II}} \right)^{2} + O\left(\frac{1}{\Omega^{2}} \right), \text{ shear,} \end{cases}$$
(20)

where n_l , n_{ll} are components of the wavenumber normals relative to the principal axes. These approximate dispersion relations, Eq. (20), generalize the longitudinal and shear dispersion relations obtained by Pierce and Kil (1990) for the particular case of a circular cylindrical shell. Equation (20) may also be obtained from Pierce's (1992a) general dispersion relation of Eq. (14) by setting $\Omega = O(k)$, with $\Omega \gg \Omega_{\rm ring}$ and $kh \ll 1$, and then expanding in $1/\Omega^2$.

Note that the effect of the fluid loading on supersonic membrane waves is to introduce attenuation, since Eq. (20) implies that Im k > 0. The damping is small over distances on the order of one wavelength, but may be appreciable over large distances of propagation.

4.2 Normal Displacement and Group Velocity. Membrane waves are longitudinal and shear because the corresponding polarization vectors, V^{α} of Eq. (18) are to leading order parallel to **n** and \mathbf{n}^{\perp} , respectively. If we let $V^{\alpha} = V^{n^{\alpha}}$ and $V^{\alpha} = V^{n^{\perp \alpha}}$ for the longitudinal and shear wave, then the associated normal displacements are, from Eq. (16),

$$\frac{W}{V} = \frac{i}{k} \left(1 + \hat{Z}_{rad} \right)^{-1}$$

$$\times \left\{ \frac{\left(\frac{n_I^2}{R_I} + \frac{n_{II}^2}{R_{II}} \right) + \nu \left(\frac{n_{II}^2}{R_I} + \frac{n_I^2}{R_{II}} \right), \text{ longitudinal,} \right.$$

$$\times \left\{ 2n_I n_{II} \left(\frac{1}{R_{II}} - \frac{1}{R_{II}} \right), \text{ shear.} \right. \tag{21}$$

Note that the normal displacement for a shear wave vanishes if the ray is parallel to a principal direction or if the curvatures are equal. Hence, W/V=0 for shear waves on a spherical thin shell. Considered as a function of propagation direction, the ratio |W/V| for longitudinal waves is greatest for propagation along the principal direction of greatest curvature and least for the other direction, while for shear waves the ratio is largest if the wave normal bisects the principal directions.

The group velocity is defined as $c_g = \partial \omega / \partial k$, and may be derived from the dispersion relations (20). For simplicity we ignore the effects of fluid loading in order to emphasize the influence of the surface curvature. Setting $\hat{Z}_{rad} = 0$ in Eq. (20) we find that

$$\mathbf{c}_{g} = \frac{k}{\omega} c^{2} \mathbf{n} + \frac{c}{k^{2}} \mathbf{n}^{\perp} \left(\frac{1}{R_{II}} - \frac{1}{R_{I}} \right) 2n_{I}n_{II}$$

$$\left((1 - \nu) \left[\frac{n_{I}^{2}}{R_{I}} + \frac{n_{II}^{2}}{R_{II}} + \nu \left(\frac{n_{II}^{2}}{R_{I}} + \frac{n_{I}^{2}}{R_{II}} \right) \right], \text{ longitudinal,}$$

$$2(n_{I}^{2} - n_{II}^{2}) \left(\frac{1}{R_{II}} - \frac{1}{R_{I}} \right), \text{ shear.}$$
(22)

Here c is the wave speed of the wave on a flat plate, i.e., c =

 c_p for longitudinal waves, and $c = c_s$ for shear waves. The component of the group velocity in the direction perpendicular to the wave normal is of order $(kR)^{-2}$, which is asymptotically small. Therefore, it should be emphasized that the correction to c_s is necessarily small.

The directional trend in the correction can be surmised from Eq. (22) by considering the case of $R_I \ge R_{II} > 0$. Clearly, c_g and n are parallel on spherical regions ($R_I = R_{II}$), and when the propagation direction is along one of the principal directions ($n_I n_{II} = 0$), or if the mode is shear and n bisects the principal directions ($n_I^2 = n_{II}^2$). Otherwise the group velocity has a non-zero component perpendicular to n. For longitudinal waves the group velocity is inclined towards the direction of higher curvature, whereas for shear waves, the group velocity is inclined away from the closest principal direction.

5 Flexural Waves

5.1 The Dispersion Relation. Let $\lambda = 1$, $\mu = 1$ in Eq. (5), and assume the flexural ansatz

$$v^{(\epsilon)\alpha}(\mathbf{x}, t) = \epsilon V^{\alpha}(\mathbf{x}, t) + \epsilon^2 \hat{V}^{\alpha}(\mathbf{x}, t) + \dots, \qquad (23a)$$

$$w^{(\epsilon)}(\mathbf{x}, t) = W(\mathbf{x}, t) + \epsilon \hat{W}(\mathbf{x}, t) + \dots$$
 (23b)

Then substitute into Eqs. (4) and isolate the leading order terms to get an algebraic system for W and V^{α} . At this stage we are finished with the scaling arguments and it is more convenient to renormalize the results which can be simply accomplished by setting $\epsilon = 1$. The system becomes

$$F_{\alpha\beta}V^{\beta} - iG_{\alpha\beta}k^{\beta}W = 0, \qquad (24a)$$

$$-iG_{\alpha\beta}k^{\beta}V^{\alpha} + \left(\Omega^2 - \Omega_{\text{ring}}^2 - \frac{h^2}{12}k^4 + \Omega^2\hat{Z}_{rad}\right)W = 0. \quad (24(b)$$

The only difference between these equations and Eqs. (14) of Pierce (1992a) is that the frequency is absent from the insurface equations.

Hence, from Eq. (24a) and the identity

$$(F^{-1})^{\alpha}_{\beta} = \frac{2}{(1-\nu)k^4} \left[k^2 a^{\alpha}_{\beta} - \frac{1}{2}(1+\nu)k^{\alpha}k_{\beta} \right], \tag{25}$$

which follows directly from the definition of F_{β}^{α} in Eq. (9a), we deduce

$$\frac{V^{\alpha}}{W} = \frac{2i}{(1-\nu)k} \left[G^{\alpha\beta} n_{\beta} - \frac{1}{2} (1+\nu) G^{\beta\gamma} n_{\beta} n_{\gamma} n^{\alpha} \right]. \tag{26}$$

Combining Eqs. (24b) and (26), and then simplifying by substituting for G^{α}_{β} and Ω_{ring} , we deduce the dispersion relation for flexural waves as

$$\Omega^{2}(1+\hat{Z}_{rad})-\frac{h^{2}}{12}k^{4}-(1-\nu^{2})(d^{\alpha\beta}n_{\alpha}^{\perp}n_{\beta}^{\perp})^{2}=0, \qquad (27)$$

or, in principal coordinates,

$$\Omega^{2}(1+\hat{Z}_{rad}) - \frac{h^{2}}{12} k^{4} - (1-\nu^{2}) \left(\frac{n_{II}^{2}}{R_{I}} + \frac{n_{I}^{2}}{R_{II}}\right)^{2} = 0.$$
 (28)

The final term introduces anisotropy, but only if $R_I \neq R_{II}$. In general, Eq. (28) determines the magnitude of the wave number k as a function of Ω and the direction of the wave normal n, i.e., $k = k(\Omega, n)$.

The dispersion relation of Eq. (28) has been previously derived by Germogenova (1973), Eq. (23), and Pierce (1992a), Eq. (72). It is important to point out that the anisotropy terms in Eq. (28) do not arise from an asymptotic expansion of the leading order dispersion relation, as was the case for the membrane waves. Thus, the terms involving curvature in the membrane dispersion relations, Eq. (20) are necessarily small by

virtue of the asymptotic scaling employed. Each term in Eq. (28) is of the same order, in principle, implying that the curvature correction is a first order effect for the flexural wave. It should be kept in mind that the asymptotic scalings for the membrane and flexure waves are slightly different. Referring to Eq. (5), we note that in the former case $\lambda = 1$ and $\mu = 0$, implying that both the frequency and wavenumber are large. This is the normal state of affairs in high frequency asymptotics when the wavenumber and frequency are proportional; if one is large the other is also. However, for the flexural waves ($\lambda = \mu = 1$) only the wavenumber is large, the frequency may be of order unity. Therefore, the final term in Eq. (28) may be of the same magnitude as the first, and the term $h^2k^4/12$ is also comparable because kh << 1 by necessity.

5.2 The Tangential Displacement. The polarization of the tangential displacement field associated with the flexural wave follows from Eq. (26), which may be expressed simply in principal coordinates in terms of components parallel and perpendicular to the wavenumber vector, as

$$\frac{\mathbf{V}}{W} = \frac{i}{k} \left\{ \left[\left(\frac{n_I^2}{R_I} + \frac{n_{II}^2}{R_{II}} \right) + \nu \left(\frac{n_{II}^2}{R_I} + \frac{n_I^2}{R_{II}} \right) \right] \mathbf{n} - 2n_I n_{II} \left(\frac{1}{R_I} - \frac{1}{R_{II}} \right) \mathbf{n}^{\perp} \right\}.$$
(29)

It is interesting to note that the polarization of the tangential displacement is not directly dependent upon fluid loading; whereas the polarization of the normal displacement for the membrane waves given by Eq. (21) does explicitly depend upon fluid loading.

Examining Eq. (29), we see that if $R_I = R_{II}$ the polarization and k are collinear, otherwise the polarization is tilted towards the direction of highest curvature. The angle between the polarization direction and the wavenumber is

$$\psi = \tan^{-1} \left\{ \frac{2n_{I}n_{II} \left(\frac{1}{R_{I}} - \frac{1}{R_{II}} \right)}{\left(\frac{n_{I}^{2} + n_{II}^{2}}{R_{I}} + \nu \left(\frac{n_{II}^{2} + n_{I}^{2}}{R_{I}} + \frac{n_{I}^{2}}{R_{II}} \right)} \right\},$$
(30)

which achieves the stationary value

$$\psi_{\text{max}} = \tan^{-1} \left\{ \frac{\frac{1}{R_I} - \frac{1}{R_{II}}}{\sqrt{\left(\frac{1}{R_I} + \frac{\nu}{R_{II}}\right) \left(\frac{1}{R_{II}} + \frac{\nu}{R_I}\right)}} \right\}, \quad (31)$$

when

$$\left(\frac{1}{R_I} + \frac{\nu}{R_{II}}\right) n_I^2 = \left(\frac{1}{R_{II}} + \frac{\nu}{R_I}\right) n_{II}^2. \tag{32}$$

If one of the curvatures is zero, then $\psi_{\text{max}} = \tan^{-1}(1/\sqrt{\nu})$, and occurs when k makes an angle ψ_{max} with respect to the direction of non-zero curvature. For steel, with $\nu = 0.289$, we find $\psi_{\text{max}} = 61.74^{\circ}$. When both curvatures are non-zero and positive, it follows from Eq. (31) that the maximum value of ψ will be less. Hence the maximum possible deviation, ψ , is achieved on regions where one of the principal curvatures vanishes. We note also from Eq. (30) that $\psi = O(1)$, and so the degree of anisotropy is independent of frequency. However, for a fixed value of W the magnitude of the tangential displacement associated with the flexural wave decreases as 1/k, from Eq. (29). At high frequencies the magnitude of k is virtually constant as a function of direction of propagation. The magnitude of the tangential displacement continues to be a strong function of propagation direction, and has a directional maximum when

$$\frac{n_{II}}{n_{I}} \approx \sqrt{\frac{\frac{1}{R_{I}} - \frac{1}{R_{II}} - \frac{(1-\nu)}{R_{II}}}{\frac{1}{R_{I}} - \frac{1}{R_{II}} + \frac{(1-\nu)}{R_{I}}}}.$$
(33)

The maximum value is

$$k \left| \frac{\mathbf{V}}{W} \right|_{\text{max}} \approx \frac{2}{\sqrt{3-\nu}} \sqrt{\left(\frac{1}{R_I} - \frac{1}{R_{II}}\right)^2 + \frac{(1+\nu)}{R_I R_{II}}}.$$
 (34)

If one of the principal curvatures vanishes, the maximum amplitude occurs at the angle $\tan^{-1} \left\{ 1/\sqrt{2-\nu} \right\}$ with respect to the direction of non-zero curvature, which is 37.40 deg for steel.

5.3 Group Velocity. The group and phase velocities follow from Eq. (28) for fluid loading. In order to simplify things we consider the case of no fluid loading, $\hat{Z}_{rad} = 0$. The group velocity, $c_g = \partial \omega / \partial k$, follows by differentiating the dispersion relation Eq. (28) and using Eq. (8a), yielding

 $\omega \rho h \mathbf{c}_g = 2Bk^2 \mathbf{k} + C(1 - v^2) 2n_I n_{II}$

$$\times \left(\frac{n_{II}^2}{R_I} + \frac{n_I^2}{R_{II}}\right) \left(\frac{1}{R_I} - \frac{1}{R_{II}}\right) \frac{\mathbf{k}^{\perp}}{k^2}. \quad (35)$$

Consider the case of $R_I > R_{II} > 0$, then Eq. (35) implies that c has a negative component in the direction of $\mathbf{k}^{\perp} = (-k_{II}, k_I)$. Hence, in general the effect of curvature is to incline the group velocity vector towards the direction of lower curvature. The size of the angle between \mathbf{n} and \mathbf{c}_g becomes independent of the frequency for high frequencies, and is solely a function of the wave normal \mathbf{n} . For instance, if one of the principal curvatures is zero, the angle is largest for \mathbf{n} oriented at 30 deg to the direction of zero curvature.

The energy flux vector on a shell has components (Pierce, 1992b)

$$\mathfrak{F}^{\alpha} = m^{\alpha}_{\beta} \ D^{\beta} \frac{\partial w}{\partial t} - \frac{\partial w}{\partial t} \ D^{\beta} \ m^{\alpha}_{\beta} - n^{\alpha}_{\beta} \frac{\partial v^{\beta}}{\partial t}. \tag{36}$$

The total energy density \mathcal{E} is the sum of the elastic energy density per unit area,

$$U = \frac{1}{2} n^{\alpha\beta} e_{\alpha\beta} - \frac{1}{2} m^{\alpha\beta} D_{\alpha} D_{\beta} w, \qquad (37)$$

plus the shell kinetic energy. In both Eqs. (36) and (37) the quantities are the real valued stresses, strains, etc. The energy propagation velocity for time harmonic motion is defined as $\mathbf{c}_{\epsilon}^{\alpha} = \langle \mathfrak{F}^{\alpha} \rangle / \langle \epsilon \rangle$, where the brackets $\langle \ \rangle$ denotes the time average over one cycle. The vector \mathbf{c}_{ϵ} can be determined by direct calculation using the same asymptotic expansion and the relation Eq. (26) for the tangential displacement components. Omitting the details, we find that

$$\langle \mathfrak{F}^{\alpha} \rangle = \frac{\omega^2}{2} \rho h |W|^2 c^{\alpha}, \quad \langle \mathcal{E} \rangle = \frac{\omega^2}{2} \rho h |W|^2,$$
 (38)

and hence we have the anticipated result, that the energy propagation velocity coincides with the group velocity, $\mathbf{c}_{\varepsilon} = \mathbf{c}_{\varepsilon}$.

6 Applications to Conical Shells

Let s, s > 0, be the distance from the vertex of the cone, and θ , $0 \le \theta \le 2\pi$, the azimuthal angle on the surface. The principal directions, I and II, may be associated with the s and θ coordinates, in which case we have $1/R_I = 0$, $R_{II} = R$, where $R = s \tan \alpha$, and α is the cone semi-angle, $0 \le \alpha \le \pi/2$. The upper and lower limits of α correspond to a flat plate, and a circular cylinder, respectively. Both limits are included in the

general analysis here, in particular, the limit of the circular cylinder is given by letting $\alpha \to 0$ while $s - z + a/\alpha$, where a is the cylinder radius and z the axial coordinate. The principal wavenumbers are $k_I = k_{\sigma}$ and $k_{II} = k_{\theta}/s \sin \alpha$.

The results in the following sections can be obtained by using the known conical shell equations of motion (Leissa, 1973), but it is perhaps more illustrative to use the previously derived approximations from the equations of motion of an arbitrarily shaped shell. Also, the effects of fluid loading will be ignored here. Our main point is to emphasize the dispersive and anisotropic effects.

6.1 Flexural Waves. The dispersion relation (28) becomes, with $\hat{Z}_{rad} = 0$,

$$\Omega^2 = \frac{h^2}{12} k^4 + (1 - \nu^2) \frac{n_s^4}{R^2}$$

$$=\frac{h^2}{12}\left(k_s^2 + \frac{k_\theta^2}{s^2\sin^2\alpha}\right)^2 + (1-\nu^2)\frac{n_s^4}{s^2\tan^2\alpha}.$$
 (39)

Since any developable surface is isometric to a plane (Struik, 1968), some conceptual simplification can be gained by considering the ray equation on the "flattened" conical surface, obtained by unfolding the cone. This can be achieved by thinking of the cone as cut along a line from the vertex, and then spread out on a plane. Since the cut is arbitrary, no discontinuity in field variables can occur as the point on the plane crosses the cut. The unfolding process has the effect of converting a conical cap into a circular segment on the plane, of interior angle $2\pi \sin \alpha$. Let x and y be coordinates on the plane spanned by the orthonormal vectors \mathbf{e}_1 and \mathbf{e}_2 , with $\mathbf{x} = x\mathbf{e}_1$

+ ye_2 , and $\hat{x} = x/s$, where $s = \sqrt{x^2 + y^2}$ is the distance from the vertex. We also define n = k/k, $k = \sqrt{k_x^2 + k_y^2}$, and $n^{\perp} = e_3 \wedge n$, where $e_3 = e_1 \wedge e_2$. The eiconal Eq. (39) becomes

$$\Omega^2 = \frac{h^2}{12} k^4 + (1 - \nu^2) \frac{(\mathbf{n}.\hat{\mathbf{x}})^4}{s^2 \tan^2 \alpha}.$$
 (40)

This dispersion relation is both anisotropic and inhomogeneous. The associated rays will not be straight lines on the flattened conical surface, which are the geodesics on the cone. The situation is analogous to an acoustic medium with variable sound speed, for which the ray paths are curved. The ray equations describe one-parameter solutions to the dispersion relation, and may be found from the Hamilton-Jacobi equations for Eq. (40) with θ^{α} and k_{α} considered as conjugate variables. Let time be the parameter defining the distance along a given ray, then the general form of the ray equations are

$$\dot{\theta}^{\alpha} = \frac{\partial \omega}{\partial k_{\alpha}}, \quad \dot{k_{\alpha}} = -D_{\alpha}\omega.$$
 (41)

Hence, the frequency is constant along a ray,

$$\dot{\omega} = \dot{\theta}^{\alpha} D_{\alpha} \omega + \dot{k}_{\alpha} \frac{\partial \omega}{\partial k_{\alpha}}$$

$$= 0. \tag{42}$$

The flexural ray equations follow from Eqs. (40) and (41) as

$$\dot{\mathbf{x}} = \frac{2}{\omega \rho h} \left[Bk^3 \mathbf{n} + \frac{C(1 - \nu^2)}{k s^2 \tan^2 \alpha} (\mathbf{n} \cdot \hat{\mathbf{x}})^3 (\mathbf{n}^{\perp} \cdot \hat{\mathbf{x}}) \mathbf{n}^{\perp} \right]$$
(43a)

$$\dot{\mathbf{k}} = \frac{C}{\omega \rho h} \frac{(1 - v^2)}{s^3 \tan^2 \alpha} (\mathbf{n} \cdot \hat{\mathbf{x}})^3 [3(\mathbf{n} \cdot \hat{\mathbf{x}}) \hat{\mathbf{x}} - 2\mathbf{n}], \tag{43b}$$

Note that the velocity along the ray is identical to the group velocity, $\dot{\mathbf{x}} = \mathbf{c}_g$. It is clear from the ray equations that

$$\overline{\mathbf{x} \wedge \mathbf{k}} = \dot{\mathbf{x}} \wedge \mathbf{k} + \mathbf{x} \wedge \dot{\mathbf{k}}$$
$$= 0, \tag{44}$$

which is equivalent to the identity $k_{\theta} = \text{constant}$. More directly, the fact that Ω given by Eq. (39) is independent of θ implies, from Eq. (41), that k_{θ} is constant along a ray but k_{s} is not. Note that Eq. (44) does not mean that the angular momentum $\mathbf{x} \wedge \mathbf{c}_{s}$ is conserved, because the velocity \mathbf{c}_{s} is not proportional to the wave normal vector. The ray equations may be recast in a universal form as follows. Define the nondimensional variables

$$\mathbf{X} = \frac{\tan \alpha}{\sqrt{1 - \nu^2}} \, \Omega \mathbf{x}, \quad \mathbf{K} = \frac{h}{(12)^{1/4} \sqrt{\Omega h}} \, \mathbf{k},$$

$$T = \frac{\tan \alpha}{2\sqrt{1 - \nu^2}} \, \frac{\sqrt{\Omega h}}{(12)^{1/4}} \, \omega t, \quad (45)$$

and also N = K/K, $S = \sqrt{X.X}$, with $\hat{X} = X/S$. Then the eiconal or dispersion relation (40) becomes

$$K^4 + \frac{(\mathbf{N}.\hat{\mathbf{X}})^4}{S^2} = 1,$$
 (46)

while the ray Eqs. (48) become

$$\frac{dX}{dT} = 2K^{3}N + 2\frac{(N.\hat{X})^{3}}{KS^{2}} [\hat{X} - (N.\hat{X})N], \qquad (47a)$$

$$\frac{d\mathbf{K}}{dT} = \frac{(\mathbf{N}.\hat{\mathbf{X}})^3}{S^3} [3(\mathbf{N}.\hat{\mathbf{X}})\hat{\mathbf{X}} - 2\mathbf{N}]. \tag{47b}$$

Note that the dependence upon the physical parameters E, ρ , ν , h, α , and ω has been eliminated through the use of the scaled variables of Eq. (45).

We now examine these equations in some detail. It follows from the analysis of Eq. (44) that $X \wedge K$ is constant on rays. Also, dot products with each of Eqs. (52) imply

$$\mathbf{K}.\,\frac{d\mathbf{X}}{dT} > 0, \quad \mathbf{X}.\,\frac{d\mathbf{K}}{dT} \ge 0. \tag{48}$$

The first inequality comes from the assumption that the wavenumber is non-zero, and means that the instantaneous ray direction has a positive component in the wave normal direction. The second relation implies that the wave number vector is "repulsed" from the origin, suggesting that rays tend to curve away from the origin. This is not always the case as we will see below: sometimes the rays are attracted towards the vertex. The reason is that the ray direction can and does diverge significantly from the wave normal. Also, very far from the origin the ray curvature must vanish as the variation in K diminishes as $1/S^3$. It also follows from Eqs. (46) and (52) that

$$\frac{1}{2} \mathbf{K}. \frac{d\mathbf{X}}{dT} + \mathbf{X}. \frac{d\mathbf{K}}{dT} = 1. \tag{49}$$

The general behavior of the rays can be understood by considering fans of rays emanating from points at different distances from the vertex $\mathbf{X}=0$. All directions are possible for \mathbf{K} if S>1, whereas if S<1 the wave normal is restricted to a cone about the azimuthal direction which diminishes in extent as the field point approaches the vertex. Let ψ denote the angle between the radius vector $\hat{\mathbf{X}}$ and \mathbf{N} , i.e., $\psi=\cos^{-1}\mathbf{N}.\hat{\mathbf{X}}$. If the distance S<1, then only wave normals such that

$$\cos^2 \psi < S, \tag{50}$$

are permissible. Figures 1 through 5 display fans for points at S = 1.1, 2, and 3. The fans are generated by allowing N to sweep out the unit circle, and the associated initial values of

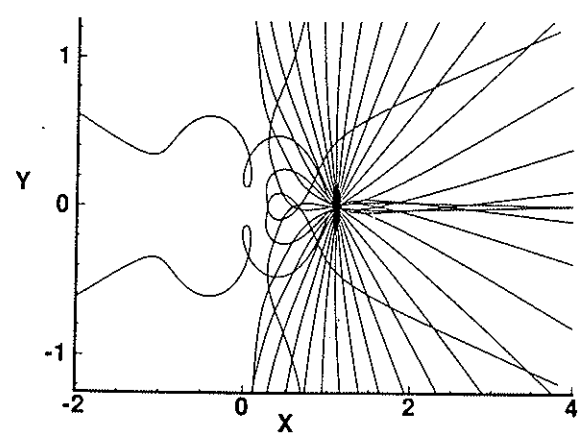


Fig. 1 Flexural rays on the universal flattened cone. The vertex lies at the origin and the source point is the S=1.1. The rays shown are for $0 \le T \le 3$ in the nondimensional units of Eqs. (45).

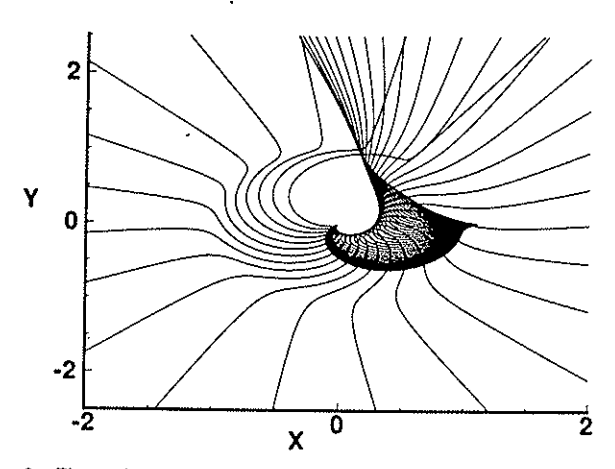


Fig. 2 Fiexural rays with N initially directed such that $140^{\circ} \leq \psi \leq 178.5^{\circ}$ where $\psi = \cos^{-1}$ N.X. Again, the starting point is at S = 1.1 and $0 \leq T \leq 3$. Note that the initial wave normals are in the second quadrant, but the rays appear to generally head into the third quadrant. The two figures differ only in the number of rays shown. The first illustrates the way in which some rays turn sharply, and the second shows the caustic formed near the vertex.

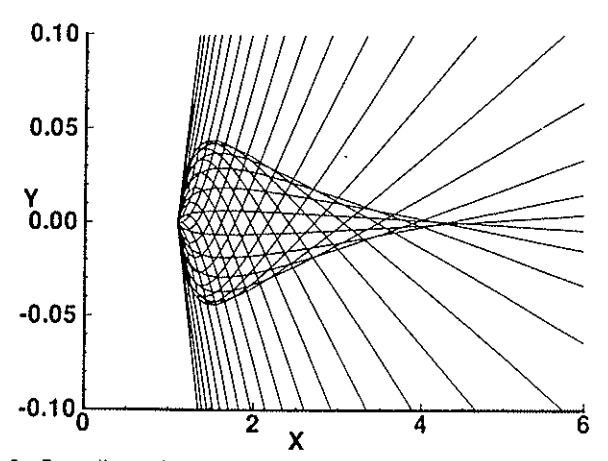


Fig. 3 Rays directed away from the vertex at the launch point S=1.1, with $-40^{\circ} \leq \psi \leq 40^{\circ}$ and $0 \leq T \leq 3$. Note that rays with initial wave normal in the first quadrant can have ray directions in the fourth quadrant. The structure of the caustic near the axis is clear from the expanded Y scale.

K follow from Eq. (46). The ray paths shown were all generated using a 4th order Runge-Kutta code. Rays initially directed away from the vertex are almost linear, and become more so as the distance increases. On the other hand, rays tending

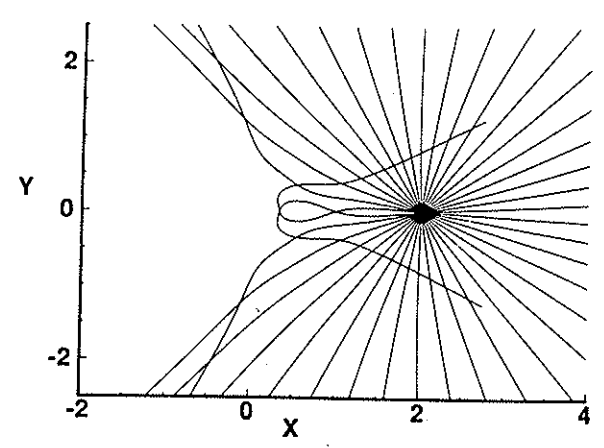


Fig. 4 Flexural rays on the flat cone for starting point at S=2 for $T<0\le 3$ and evenly space directions N on the unit circle. The caustic in the forward direction that was present for S=1.1 has now disappeared.

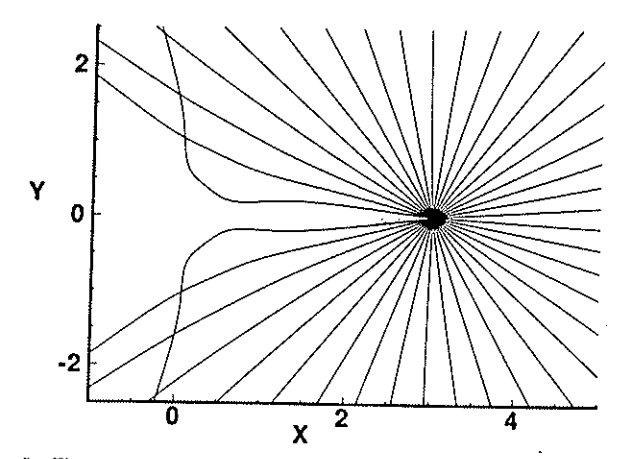


Fig. 5 The same as Fig. 4 but for S=3. The rays are clearly less anisotropic as the source point recedes from the vertex.

towards the vertex become highly distorted, and seem to behave in apparently strange ways. The behavior of the rays are dictated by the direction at which each was launched along with the radius of curvature encountered as they travel. Some rays traveling towards the vertex turn around while others bend and ultimately dive into the vertex, only to be suddenly turned backwards, and ultimately escape to infinity. Rays with this latter response form a caustic near the vertex, as displayed in Fig. 2. As S increases, the rays are generally straight lines indicating less anisotropic behavior as seen in Figs. 4 and 5.

The fact that rays sweep past the vertex and travel out to infinity can be related to the behavior of modes on a cone. Individual modes of order n can be defined by removing the azimuthal angular dependence, reducing the problem to a unidimensional inhomogeneous waveguide problem. In the high frequency limit there exists a one-to-one correspondence between the "far-field" azimuthal component of the wavenumber and the azimuthal order (n) of a mode. The turn-around of the ray can be associated with a modal cut-off, similar to the cut-off seen in wedge-like waveguides (Arnold and Felsen, 1983).

The behavior of the ray equations simplifies near the vertex. Because the dispersion relation (46) implies that $0 < K \le 1$, it also means that $N.\hat{X} \rightarrow 0$ as $S \rightarrow 0$, or more precisely

$$\mathbf{N}.\hat{\mathbf{X}} \approx \pm \sqrt{S}, \text{ as } S \to 0.$$
 (51)

The ray Eqs. (47) become

$$\frac{d\mathbf{X}}{dT} \approx \pm \frac{2}{KS^{3/2}} \,\mathbf{X}, \quad \frac{d\mathbf{K}}{dT} \approx \mp \frac{2}{KS^{3/2}} \,\mathbf{K}. \tag{52}$$

It is interesting to note that these approximate equations give $d(X \wedge K)/dT = 0$, in agreement with the exact ones, but they satisfy

$$\frac{1}{2} \mathbf{K} \cdot \frac{d\mathbf{X}}{dT} + \mathbf{X} \cdot \frac{d\mathbf{K}}{dT} \approx -1, \tag{53}$$

in contrast to Eq. (49). The difference can be explained by the asymptotic nature of Eqs. (52). Equations (52) imply that the directions of **X** and **K** are essentially constant while the magnitudes vary according to

$$\frac{dS}{dT} = \pm \frac{2}{KS^{1/2}},\tag{54a}$$

$$\frac{1}{K}\frac{dK}{dT} = -\frac{1}{S}\frac{dS}{dT}. (54b)$$

The latter equation integrates to

$$K = \frac{1}{c_0 S} \,, \tag{55}$$

and the first integrates to give

$$S = c_0^2 (T - T_0)^2, (56)$$

where c_0 and T_0 are constants. Equation (55) cannot hold for arbitrarily small S because K is bounded above by unity. The solution given by Eq. (56) is therefore only valid for some range of S small but bounded away from zero. When S becomes sufficiently small the approximation given by Eq. (51) breaks down, and the ray suddenly turns around and heads out. The + and - in Eq. (51) therefore correspond to the ray going towards and away from the vertex, respectively. It should be noted that as $S \to 0$ the magnitude of the ray velocity grows without bound, which is clearly unphysical. Far from the vertex the nondimensional speed is simply 2, but the speed of the ray in Fig. 2 that most closely approaches the vertex ($\psi = 178.5$ deg) has a maximum speed of 42, which is clearly unrealistic but nevertheless suggests that the time spent near the vertex is short in comparison to the total travel time of a ray.

Further understanding of the flexural ray paths can be gained through examining their slowness and wave surfaces. It is worth pointing out that the group velocity curve W, or the wave surface in the terminology of Musgrave (1970) is distinct from the curve P associated with constant phase, which may be defined as the envelope of the curves $k.(x-x_0) = const.$, where x_0 is the origin of phase. Thus, in an isotropic medium the curves of constant phase are circles centered at x₀. More generally, P is the polar reciprocal to the slowness surface S, which is the curve of k for fixed ω . The polar reciprocal of a curve is a purely geometrical construction (Musgrave, 1970) which maps a point on S to a point P in the direction of the normal to S at radius inversely proportional to the distance of the tangent to S from the origin. The wave surface W, on the other hand, depends not only on the shape of S at the frequency of interest, but also at neighboring frequencies, and thus is not a simple geometrical construct of S. The difference between P and W disappears if the S curves are similar, i.e. each proportional to frequency. This is the case in a nondispersive medium, as discussed by Musgrave (1970), and means for instance, that points of inflection on S become cusps on W.

The slowness surfaces for flexural waves are illustrated in Fig. 6, which shows the well-known "figure of 8" pattern (Fahy, 1985). Normally, the figure of 8's are associated with the cylindrical shell, and occur for frequencies around or below the ring frequency. The curves in Fig. 6 depend upon the position, which can be associated with frequency on an equiv-

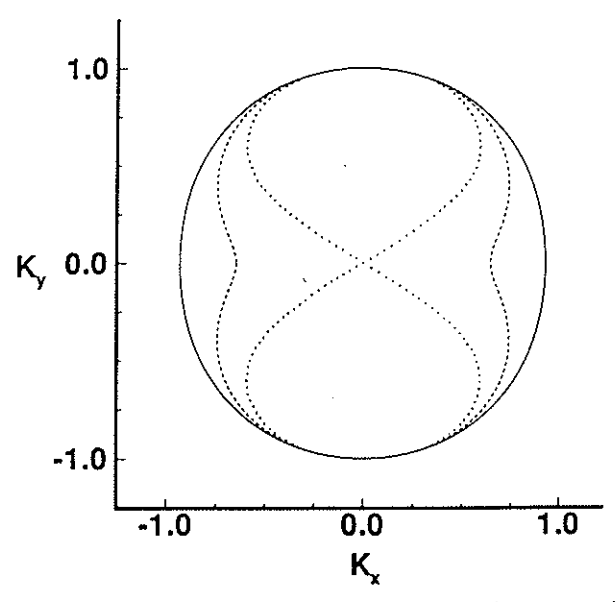


Fig. 6 Flexural slowness surfaces on the flat cone for the source point located at S equal to 0.7 (dotted line), 1.1 (dashed line), and 2 (solid line).

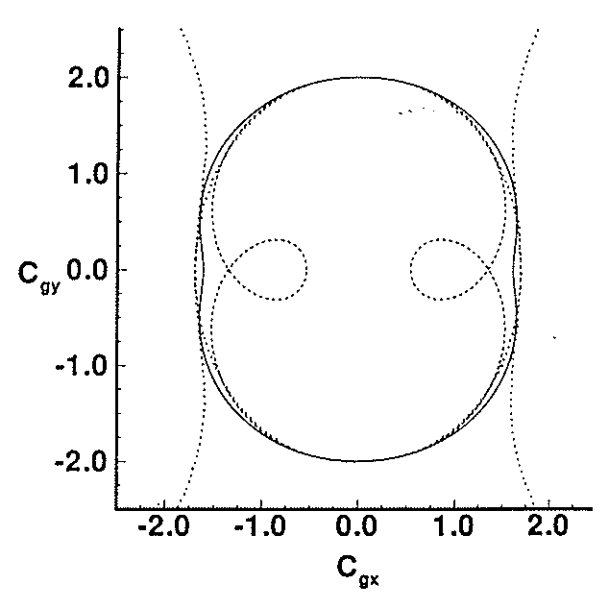


Fig. 7 Flexural wave surfaces corresponding to the slowness surfaces given in Fig. 6, from Eq. (47a). The source points are S equal to 0.7 (dotted line), 1.1 (dashed line), and 2 (solid line).

alent cylindrical shell. Thus, the value of the ring frequency depends upon one's position relative to the vertex. Referring to the discussion in the previous paragraph, we note that the wave surfaces shown in Fig. 7 are smooth and do not exhibit cusps as one would find in nondispersive media. However, the concave regions on S do correspond to multi-valued regions on the wave surfaces as seen in Fig. 7. The nonappearance of cusps on W is due to the fact, mentioned above, that the relationship of W to S is both geometrical and differential. As the vertex is approached (decreasing S), the slowness and wave surfaces become more anisotropic. If S < 1, then only wave normals satisfying Eq. (50) are permissible. When Eq. (50) is not satisfied the slowness surface has imaginary branches. Correspondingly, the wave surfaces for S < 1 are no longer closed, but have branches which tend to infinity as $K \to 0$, as exhibited by Eq. (47a).

Lastly, the polarization of the tangential displacement field for the flexural wave, given by Eq. (29), can be determined for the conical shell using $n_I - \mathbf{N} \cdot \hat{\mathbf{X}}$, $n_{II} \rightarrow -\mathbf{N}^\perp \cdot \hat{\mathbf{X}}$, as

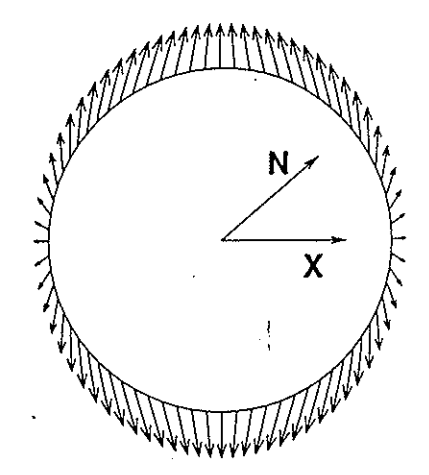


Fig. 8 The polarization of the tangential displacement associated with the flexural wave given by Eq. (57) for a conical shell. Note that the vectors indicate the magnitude and the direction of the polarization.

$$kR \frac{\mathbf{V}}{W} = i\{[(\mathbf{N}^{\perp}.\hat{\mathbf{X}})^2 + \nu(\mathbf{N}.\hat{\mathbf{X}})^2] \ \mathbf{N} - 2(\mathbf{N}.\hat{\mathbf{X}})(\mathbf{N}^{\perp}.\hat{\mathbf{X}})\mathbf{N}^{\perp}\}.$$
 (57)

This is shown in Fig. 8. As stated previously, if one of the principal curvatures is zero, then the maximum amplitude occurs at the angle $\tan^{-1}\{1/\sqrt{2-\nu}\}$ with respect to the direction of non-zero curvature, which is 37.40 deg for steel. Thus, the maximum value of the polarization from Eq. (34) is

$$kR \left| \frac{\mathbf{V}}{W} \right|_{\text{max}} \approx \frac{2}{\sqrt{3-\nu}},$$
 (58)

which is 1,214 for steel.

6.2 Membrane Waves. We now consider the behavior of membrane waves on a conical shell. The dispersion relations follow from Eq. (20) as

$$\Omega^{2} = \begin{cases} k^{2} + \frac{(n_{\theta}^{2} + \nu n_{s}^{2})^{2}}{s^{2} \tan^{2} \alpha}, & \text{longitudinal,} \\ \frac{(1 - \nu)}{2} k^{2} + \frac{(1 - \nu)}{2} \frac{(2n_{s}n_{\theta})^{2}}{s^{2} \tan^{2} \alpha}, & \text{shear.} \end{cases}$$
(59)

Once again the fact that Ω is independent of θ implies, from Eq. (41), that k_{θ} is constant along a ray but k_{s} is not. As done previously for the flexural waves, some conceptual simplification can be gained by considering the ray equation on the "flattened" conical surface. Using the same notation, the eiconal Eqs. (59) become

$$\Omega^{2} = \begin{cases} k^{2} + \frac{[1 - (1 - \nu)(\mathbf{n}.\hat{\mathbf{x}})^{2}]^{2}}{s^{2} \tan^{2} \alpha}, & \text{longitudinal,} \\ \frac{(1 - \nu)}{2} k^{2} + \frac{2(1 - \nu)}{s^{2} \tan^{2} \alpha} (\mathbf{n}.\hat{\mathbf{x}})^{2} [1 - (\mathbf{n}.\hat{\mathbf{x}})^{2}], & \text{shear.} \end{cases}$$
(60)

The ray equations follow from Eqs. (41) and (60). For the longitudinal waves, we have

$$\dot{\mathbf{x}} = c_{\rho}^{2} \frac{k}{\omega} \left\{ \mathbf{n} - \frac{2(1-\nu)}{k^{2} s^{2} \tan^{2} \alpha} [1 - (1-\nu)(\mathbf{n}.\hat{\mathbf{x}})^{2}] (\mathbf{n}.\hat{\mathbf{x}}) (\mathbf{n}^{\perp}.\hat{\mathbf{x}}) \mathbf{n}^{\perp} \right\},$$
(61a)

$$\hat{\mathbf{k}} = \frac{c_p^2}{\omega} \frac{[1 - (1 - \nu)(\mathbf{n}.\hat{\mathbf{x}})^2]}{s^3 \tan^2 \alpha} \left\{ [1 - 3(1 - \nu)(\mathbf{n}.\hat{\mathbf{x}})^2] \hat{\mathbf{x}} + 2(1 - \nu)(\mathbf{n}.\hat{\mathbf{x}}) \mathbf{n} \right\},$$
(61b)

and, similarly for the shear waves,

$$\dot{\mathbf{x}} = c_s^2 \frac{k}{\omega} \left\{ \mathbf{n} + \frac{4}{k^2 s^2 \tan^2 \alpha} \left[1 - 2(\mathbf{n} \cdot \hat{\mathbf{x}})^2 \right] (\mathbf{n} \cdot \hat{\mathbf{x}}) (\mathbf{n}^{\perp} \cdot \hat{\mathbf{x}}) \mathbf{n}^{\perp} \right\}, \quad (62a)$$

$$\dot{\mathbf{k}} = \frac{c_s^2}{\omega} \frac{4\mathbf{n}.\hat{\mathbf{x}}}{\sin^2 \alpha} \left\{ [2 - 3(\mathbf{n}.\hat{\mathbf{x}})^2] (\mathbf{n}.\hat{\mathbf{x}})\hat{\mathbf{x}} - [1 - 2(\mathbf{n}.\hat{\mathbf{x}})^2]\mathbf{n} \right\}.$$
 (62b)

Recall that in Eqs. (59) through (62), the terms involving the curvature are of lower order, namely $\epsilon^2 = h/R$. Neglecting these smaller terms, one obtains dispersion relations $\omega = ck$, where $c = c_p$ for longitudinal waves and $c = c_s$ for shear waves, which are identical to the dispersion relations for a thin flat plate. The rays are straight lines, corresponding to geodesic curves on the conical surface. The additional terms in the dispersion relations of Eq. (60) are necessarily small, on account of the scaling which led to them, and they cannot lead to any significant department from the geodesic rays. However, some idea of the qualitative behavior of the rays near the vertex can be gained by considering the exact solutions to the ray Eqs. (61) and (62), even though they may depart significantly from straight rays. In fact, we can expect the "smaller order" terms to become important as a ray approaches the vertex because the radius of curvature is small there. At the same time, the group velocities may reach unphysical magnitudes. Thus, in order to gain some insight into curvature effects on membrane waves, the smaller order ϵ^2 term will be retained subject to the constraint of meaningful group velocities.

The eiconal and ray Eqs. (60), (61) and (62) which include curvature effects can be nondimensionalized in much the same way as for the flexural rays, although in each case the non-dimensional scaling depends upon the wave type. Introduce the nondimensional variables;

$$X = -\frac{\omega}{c} x \tan \alpha, \quad K = -\frac{c}{\omega} k, \quad T = \omega t \tan \alpha,$$
 (63)

where $c = c_p$ or c_s , and define N, S, X, and $\hat{\mathbf{X}}$ as before. Then the eiconal or dispersion relation (60) becomes, for longitudinal waves

$$K^2 + \frac{1}{S^2} [1 - (1 - \nu)(\mathbf{N}.\hat{\mathbf{X}})^2]^2 = 1,$$
 (64)

and shear waves,

$$K^2 + \frac{4}{S^2} (\mathbf{N}.\hat{\mathbf{X}})^2 [1 - (\mathbf{N}.\hat{\mathbf{X}})^2] = 1.$$
 (65)

The ray equations for longitudinal waves become, using Eqs. (61),

$$\frac{d\mathbf{X}}{dT} = K\mathbf{N} - \frac{2(1-\nu)}{K S^2} (\mathbf{N}.\hat{\mathbf{X}})[1 - (1-\nu)(\mathbf{N}.\hat{\mathbf{X}})^2] [\hat{\mathbf{X}} - (\mathbf{N}.\hat{\mathbf{X}})\mathbf{N}],$$
(66a)

$$\frac{d\mathbf{K}}{dT} = \frac{1}{S^3} \left[1 - (1 - \nu)(\mathbf{N}.\hat{\mathbf{X}})^2 \right] \left\{ \left[1 - 3(1 - \nu)(\mathbf{N}.\hat{\mathbf{X}})^2 \right] \hat{\mathbf{X}} + 2(1 - \nu)(\mathbf{N}.\hat{\mathbf{X}})\mathbf{N} \right\}, \quad (66b)$$

and, similarly for shear waves, using Eqs. (62),

$$\frac{d\mathbf{X}}{dT} = K\mathbf{N} + 4 \frac{\mathbf{N}.\hat{\mathbf{X}}}{KS^2} [1 - 2(\mathbf{N}.\hat{\mathbf{X}})^2] [\hat{\mathbf{X}} - (\mathbf{N}.\hat{\mathbf{X}})\mathbf{N}], \quad (67a)$$

$$\frac{d\mathbf{K}}{dT} = 4 \frac{\mathbf{N}.\hat{\mathbf{X}}}{S^3} \left\{ [2 - 3(\mathbf{N}.\hat{\mathbf{X}})^2] (\mathbf{N}.\hat{\mathbf{X}})\hat{\mathbf{X}} - [1 - 2(\mathbf{N}.\hat{\mathbf{X}})^2] \mathbf{N} \right\}.$$
(67b)

Note that the dependence upon material parameters has been eliminated from the shear wave equations and reduced to only Poisson's ratio for longitudinal waves.

Figures 9 and 10 illustrate ray traces with a source point located at S = 2 for longitudinal and shear waves, respectively. Once again the fans are generated by allowing N to sweep out

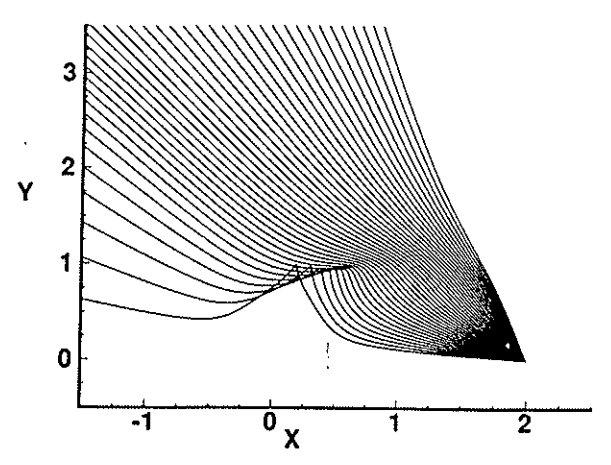


Fig. 9 Longitudinal rays on the universally flattened cone with N initially directed such that 115° $\leq \psi \leq$ 175°. The vertex lies at the origin and the source point is S=2. The rays are shown for $0 \leq T \leq 6$ in the nondimensional units of Eqs. (66). Note how the rays curve around the vertex.

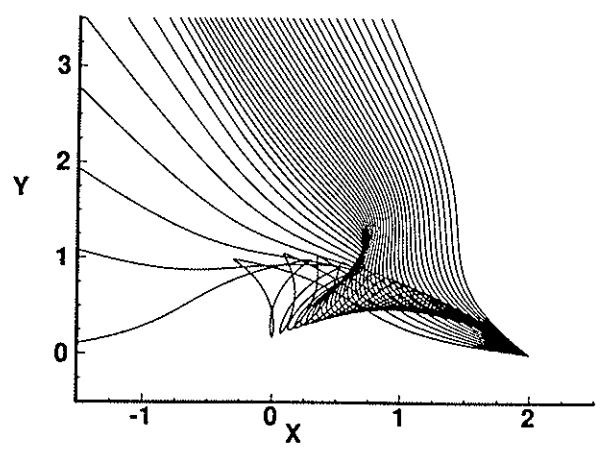


Fig. 10 Shear rays with the same parameters as Fig. 9 using the nondimensional Eqs. (67). In this instance, the rays curve into the vertex, spin around it abruptly with near approach, then head out along a curved path. Also, caustics are generated incoming to and outgoing from the vertex.

the unit circle, and the associated initial values of K follow from Eqs. (64) and (65). Longitudinal or shear rays that are initially directed away from the vertex are virtually straight. As the longitudinal rays approach the vertex they swing quickly around it before continuing on straight paths. The effect of decreasing curvature has a greater effect on the shear rays. They curve directly towards the vertex forming a caustic. At closest approach, they twist about sharply and leave the vertex along curved paths once more forming a caustic. Finally, the shear rays move on to infinity along straight trajectories.

We note from Figs. 11 and 12 that the slowness surfaces for longitudinal and shear waves have inflection points which generate smoothly varying multi-valued regions in the wave surfaces given by Eq. (66a) for longitudinal waves in Fig. 13 and given by Eq. (67a) for shear waves in Fig. 14. This is representative of a dispersive medium. The anisotropy, indicated by the extent or size of the multi-valued regions, increases as S decreases. If S < 1 for either wave type, the slowness surface has imaginary branches and the wave surface is an open curve. The open branches of the wave surface, or group velocity curve, tend to infinity as $K \to 0$, as exhibited by Eq. (66a) for longitudinal waves and Eq. (67a) for shear waves.

Finally, the magnitude of the normal displacements associated with the membrane waves are given by Eq. (21), which simplifies for the conical shell without fluid loading to

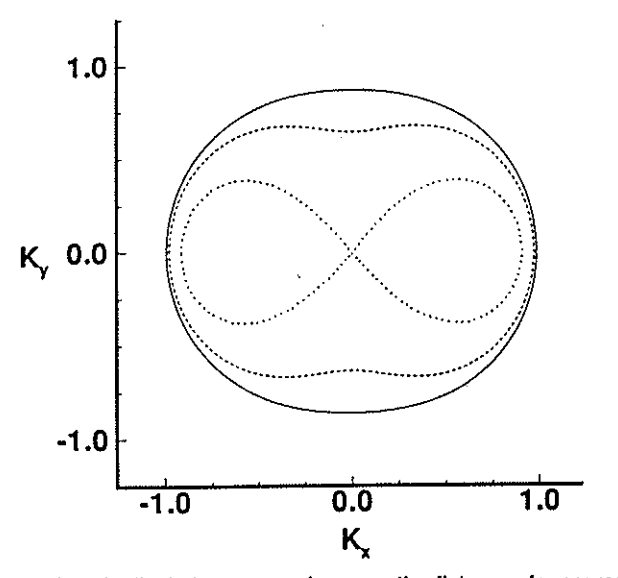


Fig. 11 Longitudinal slowness surfaces on the flat cone for source points located at S equal to 0.7 (dotted line), 1.3 (dashed line), and 2 (solid line). Note the appearance of "figure of 8" patterns (Fahy, 1985) as seen previously for flexural waves in Fig. 6.

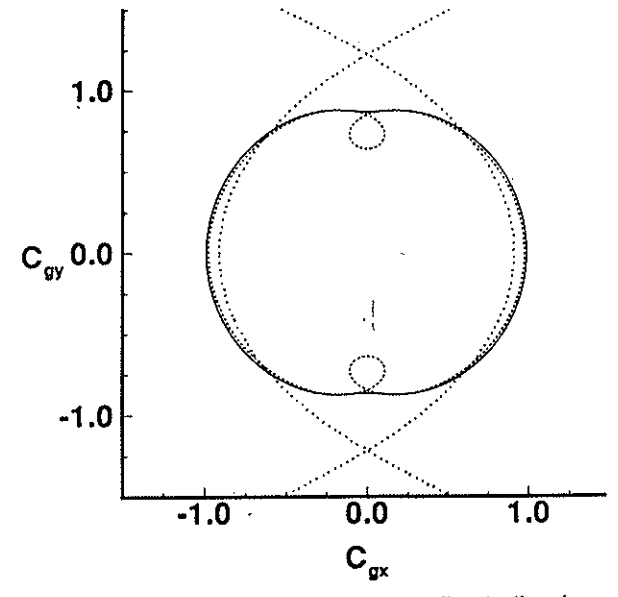


Fig. 13 Longitudinal wave surfaces corresponding to the slowness surfaces given in Fig. 11 for the source points located at S equal to 0.7 (dotted line), 1.3 (dashed line), and 2 (solid line)

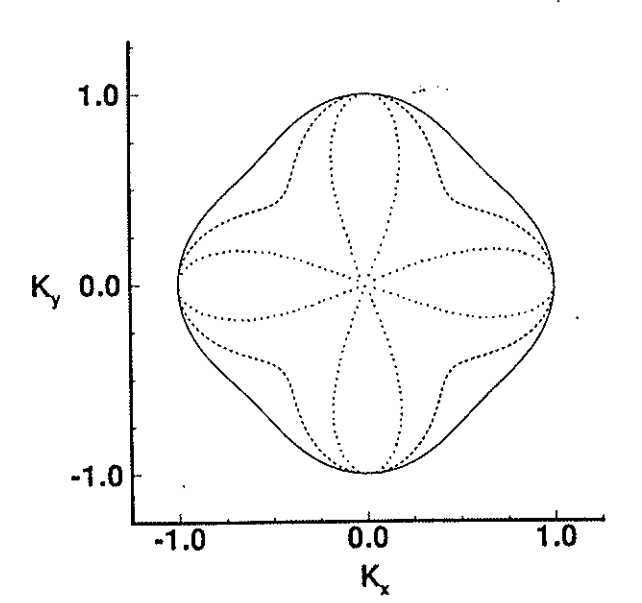


Fig. 12 Shear slowness surfaces on the flat cone for source points located at S equal to 0.7 (dotted line), 1.3 (dashed line), and 2 (solid line)

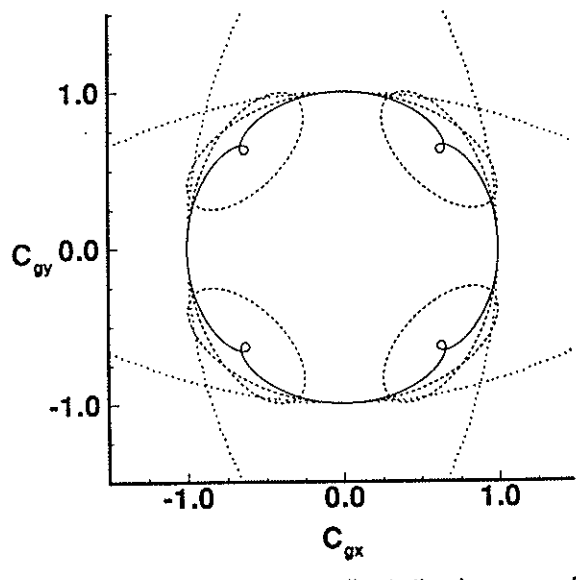


Fig. 14 Shear wave surfaces corresponding to the slowness surfaces given in Fig. 12 for the source points located at S equal to 0.7 (dotted line), 1.3 (dashed line), and 2 (solid line)

$$kR \frac{W}{V} = i \begin{cases} (\mathbf{N}^{\perp} . \hat{\mathbf{X}})^2 + \nu (\mathbf{N} . \hat{\mathbf{X}})^2, & \text{longitudinal,} \\ -2(\mathbf{N} . \hat{\mathbf{X}})(\mathbf{N}^{\perp} . \hat{\mathbf{X}}), & \text{shear.} \end{cases}$$
 (68)

These are shown in Fig. 15. It is seen that the normal displacement of the shear wave vanishes if the ray is parallel to a principal direction, and that the maximum value is unity for both cases.

7 Conclusions

We have derived asymptotic results for waves on arbitrarily curved thin shells, based upon the assumption that the wavelengths are short compared to the minimum radius of curvature. The scalings imply distinct asymptotic behavior for membrane (longitudinal and shear) and flexural waves, and lead to relatively simple formulae for the dispersion relations and associated physical quantities, such as group velocity and polarization. Some general results for flexural waves include:

- (1) The tangential polarization is parallel to the wave normal on spherical regions, otherwise,
- (2) The polarization is tilted towards the direction of highest curvature, and the deviation from n will be greatest on regions of zero Gaussian curvature.
- (3) The effect of shell curvature is to incline the group velocity towards the direction of lowest curvature.

The main results for membrane waves are

- (1) The normal displacement for a shear wave vanishes if the wave normal n is parallel to a principal direction or if the shell is locally spherical.
- (2) The ration |W/V| for longitudinal waves is greatest for propagation along the direction of greatest curvature and least for the other direction, while for shear waves the ratio is largest if the wave normal bisects the principal directions.
- (3) The group velocity is parallel to the wave normal if the shell is locally spherical, or the propagation is along one of

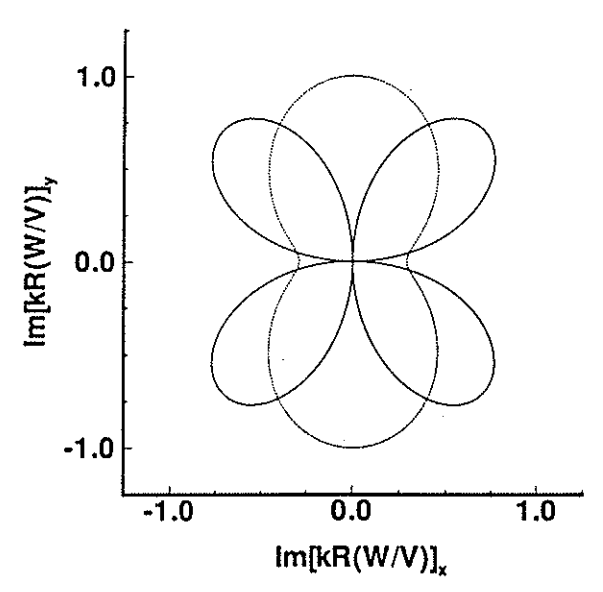


Fig. 15 The normal displacement for a conical shell associated with the longitudinal wave (dashed line) and the shear wave (solid line), as given by Eq. (68)

the principal directions, or the mode is shear and n bisects the principal directions.

(4) Otherwise, the group velocity is inclined towards the direction of higher curvature for longitudinal waves, and away from the closest principal direction for shear waves.

In general, membrane waves are weakly affected by the shell curvature, whereas flexural waves can be strongly influenced.

The ray methods developed here can serve as a tool for treating scattering and radiation from fluid-loaded shells of complex shape. We have not dealt with the issues of coupling and decoupling of the shell waves, which need to be included for a complete treatment. Some of these missing links are addressed in detail in a separate paper (Norris and Rebinsky, 1993) where practical applications are also discussed.

Acknowledgment

This work was supported by the Office of Naval Research under the supervision of Dr. G. Main.

References

Arnold, J. M., and Felsen, L. B., 1983, "Rays and Local Modes in a Wedge-Shaped Ocean," *Journal of the Acoustical Society of America*, Vol. 73, pp. 1105-1119.

Fahy, F., 1985, Sound and Structural Vibration, Academic Press, New York, pp. 200-210.

Germogenova, O. A., 1973, "Geometrical Theory of Flexure Waves in Shells," Journal of the Acoustical Society of America, Vol. 53, pp. 535-540.

Green, A. E., and Zerna, W., 1968, Theoretical Elasticity, 2nd edition, Oxford University Press, London.

Junger, M. C., and Feit, D., 1986, Sound, Structures, and Their Interaction, MIT, Cambridge, MA.

Keller, J. B., 1978, "Rays, Waves and Asymptotics," Bulletin of the American

Mathematical Society, Vol. 84, pp. 727-750.

Koiter, W. T., 1960, "A Consistent First Approximation in the General Theory of Thin Elastic Shells," The Theory of Thin Elastic Shells, W. T. Koiter, ed.,

North-Holland, Amsterdam; pp. 12-33.

Leissa, A. W., 1973, Vibrations of Shells, NASA Report SP-288.

Musgrave, M. J. P., 1970, Crystal Acoustics, Holden-Day, San Francisco.

Norris, A. N., and Rebinsky, D. A., 1994, "Acoustic Coupling to Membrane Waves on Elastic Shells," *Journal of the Acoustical Society of America*, Vol. 95, pp. 1804-1829.

Pierce, A. D., 1989, "Wave Propagation on Thin-Walled Elastic Cylindrical Shells," *Elastic Wave Propagation*, M. F. McCarthy and M. A. Hayes, eds., North-Holland, Amsterdam, pp. 205-210.

Pierce, A. D., 1992a, "Waves on Fluid-Loaded Inhomogeneous Elastic Shells of Arbitrary Shape," Structural Acoustics, R. F. Keltie et al., eds., ASME, New York, NCA-Vol. 12/AMD-Vol. 128, pp. 195-201.

York, NCA-Vol. 12/AMD-Vol. 128, pp. 195-201.
Pierce, A. D., 1992b, "Variational Formulations in Acoustic Radiation and Scattering," *Physical Acoustics*, A. D. Pierce and R. N. Thurston, eds., Academic Press, San Diego, Vol. 22, pp. 195-371.

Pierce, A. D., and Kil, H.-G., 1990, "Elastic Wave Propagation from Point Excitations of a Cylindrical Shell," ASME JOURNAL OF VIBRATION AND ACOUSTICS, Vol. 112, pp. 399–406.

Ross, E. W., 1968, "On Inextensional Vibrations of Thin Shells," ASME Journal of Applied Mechanics, Vol. 35, pp. 516-523.

Struik, D. J., 1968, Lectures on Differential Geometry, Dover, New York. Williams, E. G., Houston, B. H., and Bucaro, J. A., 1990, "Experimental Investigations of the Wave Propagation from Point Excitations on Thin-Walled Cylindrical Shells," Journal of the Acoustical Society of America, Vol. 87, pp. 513-522.

Table of Contents (continued)

573 Isolation of the Spectrograms and Rosettes of Insonified Sets of Submerged, Concentric, Thin Shells G. C. Gaunaurd and A. Akay

TECHNICAL BRIEF

578 Operation of an Electromagnetic Eddy-Current Damper with a Supercritical Shaft J. R. Frederick and M. S. Darlow

425, 448 Honors and Awards